

Shallow structure of the Yadong-Gulu rift, southern Tibet, from refraction analysis of Project INDEPTH common midpoint data

Michael J. Cogan,^{1,2} K. D. Nelson,¹ W. S. F. Kidd,³ Changde Wu,¹ and Project INDEPTH Team⁴

Abstract. Refracted arrivals on International Deep Profiling of Tibet and the Himalaya (INDEPTH) common midpoint (CMP) data provide insight into the shallow structure of the Yadong-Gulu rift in southern Tibet. This is the first such information available for the Neogene-Quaternary rifts on the Tibetan Plateau. Geologic cross sections across three separate valleys within the rift have been constructed from these data and available surface geological information. In each case, the valleys are floored by asymmetric, low-velocity sedimentary fills ranging from ~100 m to ~1.5 km in thickness. Beneath all three, the basement appears to dip gently to the east (~5°). Seismic reflection data from one of these valleys (Nyingzhong) show a ~30° east dipping reflector within the basement beneath the valley that projects upward to the normal-sense Nyainqentanglha detachment exposed in the range immediately to the west. Field investigations by INDEPTH personnel have additionally shown the existence of previously unrecognized normal-sense shear zones bordering the other two valleys. The newly discovered shear zones are 200 to >500 m thick and in both instances are characterized by moderately to steeply west dipping mylonites with top-to-west shear sense. Metamorphic minerals within the shear zones indicate at least amphibolite grade metamorphism with increasing metamorphic grade down section. The seismic data, coupled with the new geologic information and geomorphologic data from Landsat imagery, suggest that the structure of the northern Yadong-Gulu rift is comparable to other well-documented rift systems in which steep range-front normal faults terminate at, or sole into, moderately dipping normal-sense detachments at depth that have undergone substantial footwall uplift and rotation during extension. This geometry implies that the extension of the Tibetan Plateau crust has been accommodated at depth by lateral flow within the middle crust. It also suggests that E-W extension of the plateau may have been substantially greater than has generally been presumed.

1. Introduction

A notable aspect of the Himalayan collision zone is the existence of extensional rifts within the Tibetan Plateau that are forming concurrently with N-S convergence between India and Asia [Molnar and Tapponnier, 1978; Armijo *et al.*, 1986]. The relationship between horizontal shortening, up-lift, and crustal extension is currently being examined in a number of orogenic belts around the world and is thought to be fundamental to both the mechanics of collisional orogeny [e.g., Mercier *et al.*, 1987; England and Houseman, 1989] and its possible effect on global climate [e.g., Harrison *et al.*, 1992; Molnar *et al.*, 1993]. The Himalaya/Tibetan Plateau region, representing the type example of an active continent-continent collision, provides a natural laboratory within which to examine this relationship.

N-S trending grabens and half grabens and conjugate NW-SE and NE-SW trending transcurrent faults constitute direct evidence for Neogene/Quaternary extension of the Tibetan Plateau [Armijo *et al.*, 1986, 1989]. Both types of structures are spectacularly displayed on digital topographic and Land-sat images of the plateau [Armijo *et al.*, 1986, 1989; Fielding *et al.*, 1994], and examples of both have been investigated in the field by western and Chinese geologists [e.g., Armijo *et al.*, 1986, 1989; Burchfiel *et al.*, 1991]. The grabens and half grabens on the southern Tibetan Plateau are arrayed in echelon in a series of approximately N-S trending rifts [Armijo *et al.*, 1986] (Figure 1). These rifts are up to 300 km long, terminate at strike-slip faults in the center of the plateau, and appear to die out on the south flank of the Himalaya. The individual graben and half graben valleys that comprise the rifts are generally a few to ~15 km wide and continuous for several tens of kilometers. The valleys are floored by Quaternary alluvium and/or glacial till and are bordered by mountains composed variously of sedimentary, igneous, and metamorphic bedrock of Paleozoic-Cenozoic age [Liu, 1988].

In 1992 and 1994, the International Deep Profiling of Tibet and the Himalaya (INDEPTH) project acquired common-midpoint (CMP) seismic reflection data along a series of profiles within the Yadong-Gulu rift, one of the largest of the extensional rifts in Tibet (Plate 1). INDEPTH is a multi component geophysical and geological investigation of the Tibetan Plateau being undertaken collaboratively by investigators from the Chinese Academy of Geological Sciences and several North American and European geoscience institutions. The seismic data acquisition program was designed primarily to image the deep structure of the crust and uppermost mantle beneath the region but also yielded information on the Yadong-Gulu rift basin(s), which lie within the uppermost crust, principally in the form of refracted arrivals (first breaks) contained

¹Department of Earth Sciences, Syracuse University, Syracuse, New York.

²Now at Schlumberger Geco-Prakla, Houston, Texas.

³Department of Earth and Atmospheric Sciences, SUNY at Albany, Albany, New York.

⁴Additional members of the Project INDEPTH Team contributing to this research include: Wenjin Zhao, Yongjun Yue, Jixiang Li, Chinese Academy of Geological Sciences; L.D. Brown, M.L. Hauck, D. Alsdorf, M. Clark, Institute for the Study of the Continents, Cornell University; M.A. Edwards, Department of Earth and Atmospheric Sciences, SUNY at Albany; J. T. Kuo Aldridge Laboratory of Applied Geophysics and Lamont-Doherty Earth Observatory of Columbia University. Copyright 1998 by the American Geophysical Union.

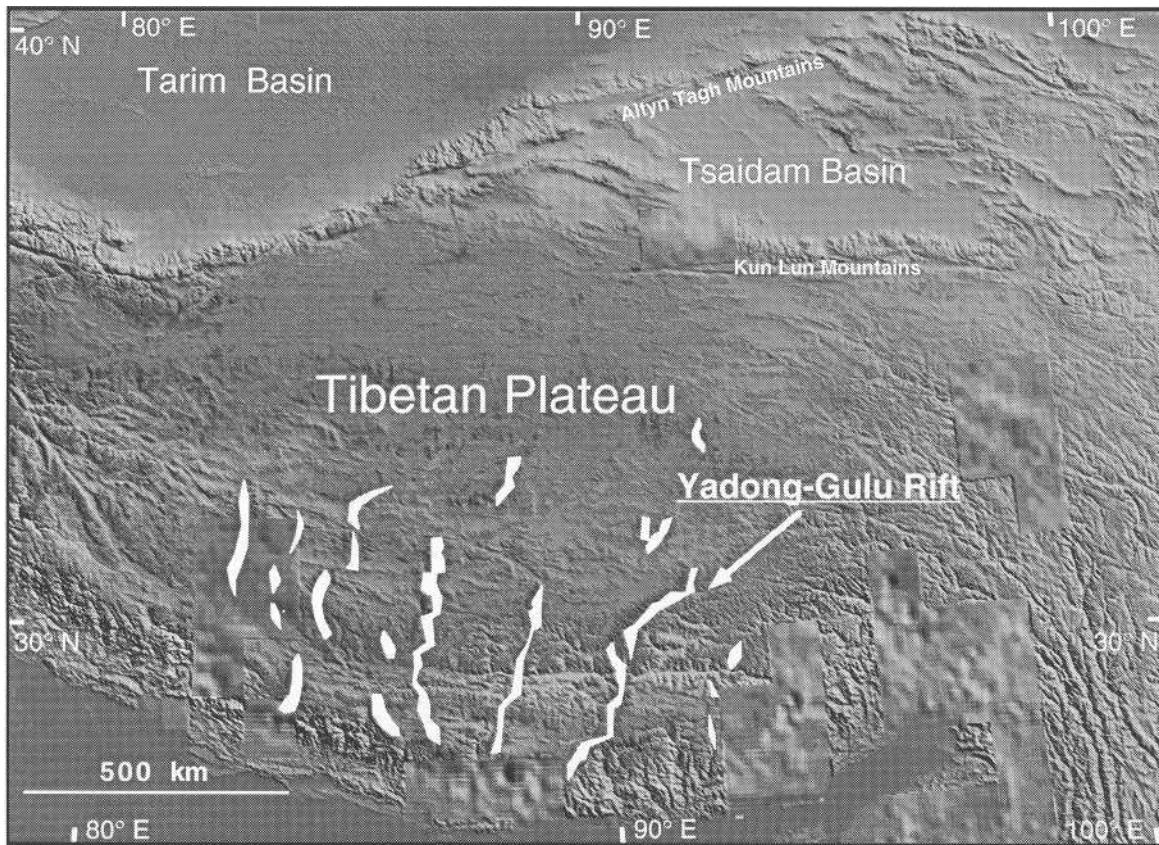


Figure 1. Digital elevation model of the Tibetan Plateau produced from data described in *Fielding et al.*, [1994]. The principal north-south trending Neogene/Quaternary rifts on the Tibetan Plateau are highlighted in white.

within the data. This paper presents an analysis of these shallow data along four crosslines acquired within the rift. These are the first such data to be acquired within a Tibetan rift. The results are then integrated with available surface geologic and remote-sensing data to produce five interpretive geologic cross sections across the rift. The seismic reflection observations relating to the deep structure of the crust and uppermost mantle beneath the region are presented elsewhere [*Zhao et al.*, 1993; *Als Dorf et al.*, 1996; *Brown et al.*, 1996; *Nelson et al.*, 1996].

2. Yadong-Gulu Rift

Owing to the large areal extent of the Tibetan Plateau and a history of restricted access, few of the Tibetan rifts have been examined closely, and only small segments have been studied in detail. The Yadong-Gulu rift which extends across south-ern Tibet at approximately 90°E longitude is the most intensively studied. The rift extends across the High Himalaya and Yarlung Zangbo suture, the latter coinciding approximately with the Yarlung Zangbo (Yarlung River) (Plate 1). North of the High Himalaya and south of the suture, the bedrock consists principally of Paleozoic-Mesozoic sedimentary strata of the Tethyan Series, representing the deformed pre-Eocene northern passive margin of India [*Gansser*, 1964; *Burg et al.*,

1984; *Searle et al.*, 1987]. Local outcrops of high-grade metamorphic rock, thought to represent deformed Indian basement (e.g., Kangmar dome), and Neogene granites also crop out in the region [*Burg et al.*, 1984; *Maluski et al.*, 1988]. Bedrock north of the suture consists principally of Cretaceous-Tertiary granodiorites and associated volcanic cover rocks of the Gangdese batholith and, farther north, Paleozoic metamorphic basement and Paleozoic-Mesozoic sedimentary cover of the Lhasa block [*Kidd et al.*, 1988].

Published information on the structure of the Yadong-Gulu rift derives largely from pioneering field investigations undertaken during the 1981-1983 Sino-French expedition to Tibet [*Amijo et al.*, 1986, 1989; *Tapponnier et al.*, 1986], supplemented by several subsequent local investigations [*Burchfiel et al.*, 1991; *Pan and Kidd*, 1992; *Ratschbacher et al.*, 1994; *Harrison et al.*, 1995]. *Amijo et al.* [1986] describe the grabens and half grabens comprising the Yadong-Gulu rift and its sister rifts as young features bounded by steeply dipping (45°-60°) planar normal faults. Normal faults are recognized in the field and on satellite images by triangularly faceted mountain fronts, prominent fault-line scarps, and truncated or displaced moraines and alluvium. Interpretive E-W cross sections drawn by *Amijo et al.* [1986] across the Yadong-Gulu rift are reproduced in Figure 2. On the basis of their surface observations, these workers argued that the Tibetan rifts, in

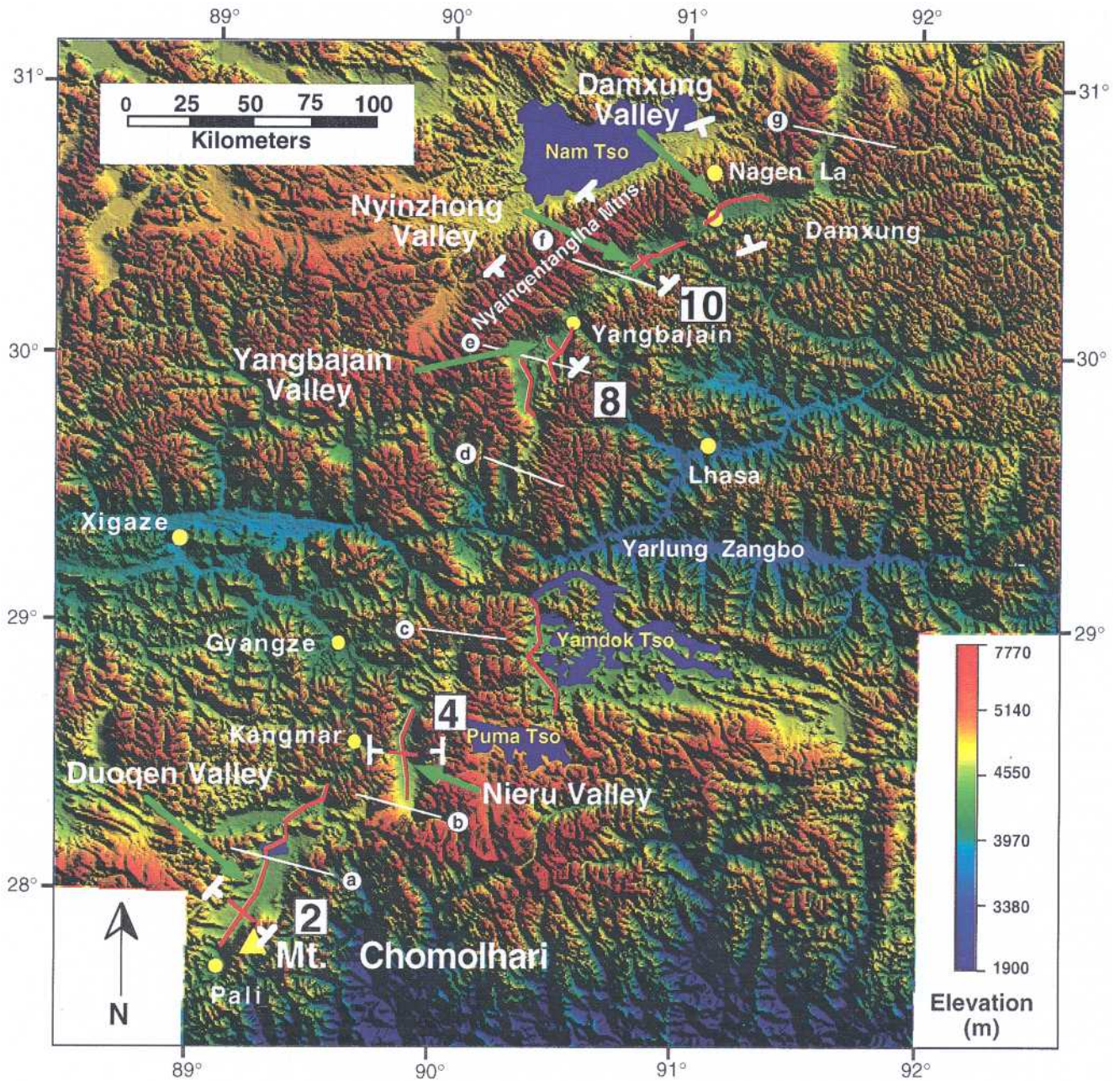


Plate 1. Digital elevation model of the Yadong-Gulu rift area produced from data described in *Fielding et al.*, [1994]. INDEPTH seismic lines are indicated by red lines. Numbered seismic lines refer to crosslines Tib-2, Tib-4, Tib-8, and Tib-10 discussed in text. Bold white reference marks indicate positions of interpretive geologic cross sections shown in Figure 8. Fine white lines with lower case letters indicate approximate positions of interpretive geologic cross sections of *Armijo et al.* [1986] reproduced in Figure 2 (see *Armijo et al.* [1986] for precise locations).

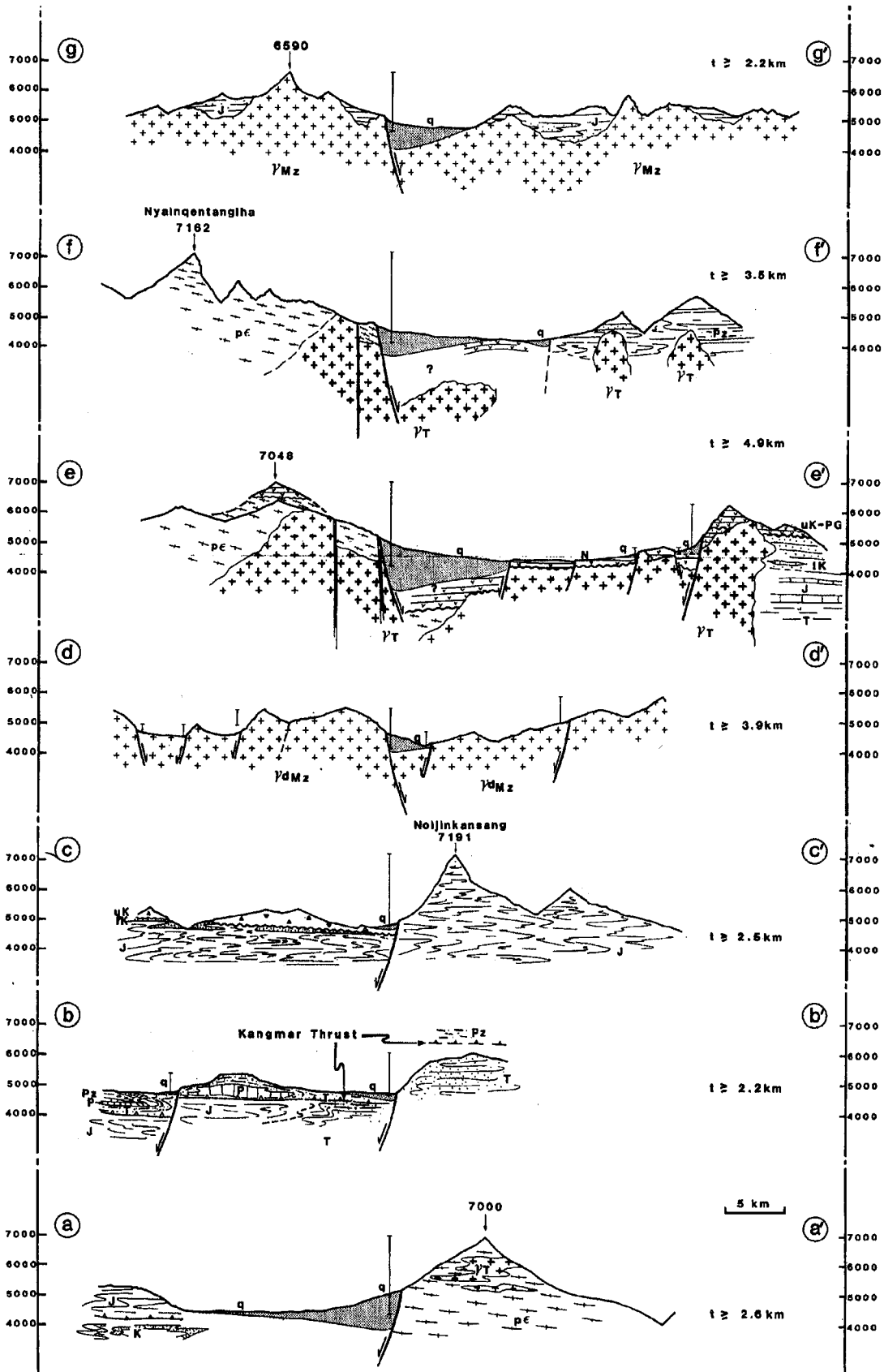


Figure 2. Interpretative cross sections across the Yadong-Gulu rift, reproduced from Armijo *et al.* [1986, plate 2]. Approximate locations of cross sections shown in Plate 1 (see Armijo *et al.* [1986] for precise locations).

general, are relatively shallow features (<1 km sedimentary fill) formed by slip on high angle normal faults and in aggregate manifest only minor east-west extension of the Tibetan Plateau (~2%).

Recent observations by *Pan and Kidd* [1992] and *Harrison et al.* [1995], as well as new geological field observations reported here, suggest that this general view may need modification. *Pan and Kidd* [1992] identified a several hundred meter thick, gently southeast dipping ductile high strain zone in the central Nyainqentanglha range bordering the northwest side of the northern Yadong-Gulu rift (Nyingzhong valley, Plate 1). This mylonite zone, termed the "Nyainqentanglha Shear Zone" (NSZ) by Pan and Kidd, exhibits well-developed S-C fabric indicating normal-sense (top to the SE) shear. *Harrison et al.* [1995] have reported $^{40}\text{Ar}/^{39}\text{Ar}$ thermochronological modeling results for samples collected in the footwall of the NSZ, which suggest that the footwall of the NSZ exposed in the central Nyainqentanglha range began to cool rapidly at about 8 Ma and that it has been uplifted (denuded) approximately 17 km since that time. As outlined subsequently, these observations can be integrated with INDEPTH geophysical and geological observations in a "core complex-type" interpretation implying several tens of kilometers extension across the northern Yadong-Gulu rift. In the southern Yadong-Gulu rift, geological investigation undertaken during the INDEPTH field program has revealed the local presence of ductile high-strain zones exhibiting normal-sense shear (top to the west) on the east side of Nieru valley ("Gabo valley" of *Burchfiel et al.*, [1991]) and the east side of Duoqen valley. The ductile high-strain zone observed on the east side of Nieru valley has been described by *Kidd et al.* [1995] and termed by them the "East Nieru Detachment" (END). The ductile high strain zone on the east side of Duoqen valley coincides with the west flank of the NNE-trending Chomolhari segment of the High Himalaya and is described by Wu et al. [this issue]. In both cases, the high-strain zones are several hundred meters thick, dip moderately to steeply west, expose garnet-grade rocks, and exhibit shear-sense indicators showing down-to-the-west (normal sense) shear. Although the age and amount of slip accommodated by these mylonite zones are unknown, their locations and shear sense imply that, like the NSZ, they are probably associated with the opening of the Yadong-Gulu rift. These field observations are incorporated in the interpretations that follow.

3. Refraction Analysis of INDEPTH Seismic Data

INDEPTH acquired approximately 300 km of CMP-type multichannel seismic data comprising eleven lines spaced along the Yadong-Gulu rift. Four of these lines are relatively short crosslines designed primarily to give three-dimensional control on the geometry of deep reflections observed on the rift-parallel lines (Tib-2, Tib-4, Tib-8, and Tib-10 in Plate 1). The seismic lines were acquired with 120-channel (Tib-1, and Tib-2) and 240-channel (Tib-3 through Tib-11) recording systems, 50-m (Tib-1 and Tib-2) and 25-m (Tib-3 through Tib-11) geophone group intervals, 200-m shot interval, and nominal 50-kg shots.

Examination of the individual shot records shows that the first arrivals are generally characterized by two legs (Figure 3). The near-source leg typically has apparent velocities of 2.4 ± 0.2 km/s. Subsequent legs typically show apparent velocities increasing from 3.5 km/s to as much as 5.7 km/s. Reference to tabulations of rock velocities measured in the laboratory indicate that the 2.4 km/s apparent velocity is appropriate for weakly consolidated sands and gravels and that the velocities in excess of 4.5 km/s are appropriate for well-indurated sedimentary and crystalline rocks [e.g., *Press*, 1966]. The 2.4-km/s arrival is therefore interpreted to be the direct arrival through the Neogene-Quaternary sedimentary fill of the rift basins. The faster arrivals observed at longer offsets are interpreted to be refracted ("head wave") arrivals through the underlying bed-rock. The shot files locally exhibit hyperbolic reflections in the upper 0 to -1.2 s that are reflections from within and/or the base of the Neogene-Quaternary basin fill and in some cases deeper reflections originating from structures within the basement.

Calculation of the depth to the basement beneath representative shots, assuming a horizontal interface, indicates that the low-velocity fill within the Yadong-Gulu rift reaches a maximum thickness of only about 1.5 km and over much of the rift is less than a few hundred meters thick thus confirming *Armijo et al.*'s [1986] general inference of a shallow rift fill. The corresponding near-vertical incidence reflection time to the base of the fill in the deepest part of the rift is therefore only about 1.25 s and for most of the rift is less than a few 100 ms. Because the rift fill is so shallow relative to the spread length (6 km) and near-trace offset (200 m) employed in the INDEPTH survey, which were optimized for imaging the deep crust, it is not imaged by standard CMP reflection processing along most of the survey. Reflections from within and/or the base of the fill are limited to the upper few 100 ms of data on the near-source traces (at larger offset, high-amplitude direct arrivals superpose them). After refraction and normal-move-out-stretch muting, which are standard steps in CMP reflection processing, these data are largely lost. Because the standard reflection processing of the INDEPTH data does not usefully image the rift fill along most of the survey, an analysis of the refracted (first) arrivals was undertaken to provide insight into the thickness and geometry of the rift fill. The analysis concentrated on the four crosslines in the INDEPTH data set (Tib-2, Tib-4, Tib-8, and Tib-10). Initial models were constructed from inverse calculations of the refracted arrivals on individual shots. These initial models were subsequently used as the starting point for forward ray trace modeling of the refracted arrivals from selected shots to produce refined models of the basin geometries along the crosslines.

3.1. Inverse Calculations

In order to get an initial estimate of the geometry and depth of the basin fill along the crosslines, projected t intercept times (time that the projected refraction crosses zero offset) of the basement refraction and apparent velocities of the basin fill and basement refractor were picked by hand from selected shot files along each line. The shot files had only limited processing applied (geometry installation, elevation statics, and gain balancing). In general, the refractor velocities appear to be reproducible to within 0.2 km/s, and t intercept times appear to

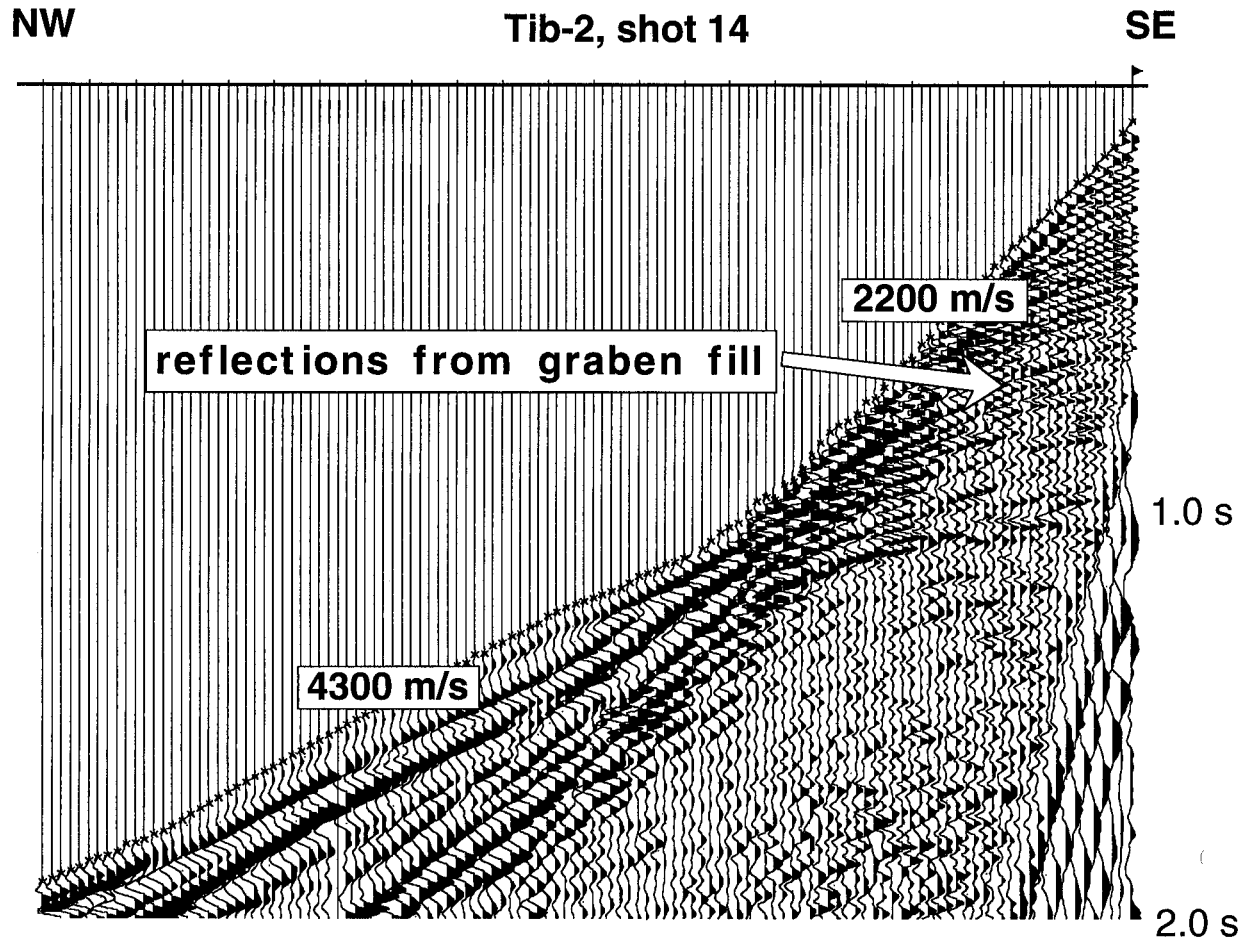


Figure 3. Sample shot record from line Tib-2 in Duoqen valley showing distinct first and second legs to the first arrival. In the area where this shot was recorded, the low-velocity graben fill is relatively thick. Over most of the Yadong-Gulu rift, the low-velocity (~ 2200 m/s) direct arrival is limited to a relatively few near traces, and reflections from within the graben fill are not clearly imaged on INDEPTH stacked seismic sections owing to the shallowness of the graben fill and 200-m near-trace offset. Trace spacing in this shot gather is 50 m.

be reproducible to within a few tens of milliseconds. These data were utilized in simple horizontal-layer refraction models to calculate an apparent depth to the refracting layers underlying each shot (Figure 4).

The inverse calculations for Tib-2, Tib-4, and Tib-10 show two identifiable layers (Figures 4d, 4c, and 4a respectively), while Tib-8 shows three layers (Figure 4b). Average interval velocities in all of the sections range from 2.2 to 2.8 km/s for the top layer, which is here interpreted to be loosely consolidated Neogene-Quaternary fluvial-glacial sands, gravels, and conglomerates comprising the rift basin fill. This material is exposed on the rift valley floors and along their margins. The second layer on lines 2 and 4 has a refraction velocity of ~ 4.5 km/s, corresponding to the velocity range of well-indurated sedimentary rocks, including sandstone, slate, and limestone. These are the predominant rock types comprising the Tethyan sedimentary series bordering the southern Yadong-Gulu rift. The second layer on lines 8 and 10 in the northern Yadong-Gulu rift exhibits somewhat lower velocity (~ 4.0 km/s) than the second layer on the lines to the south. Tib-8 (south Yangbajain)

shows a substantially higher-velocity third layer (~ 5.7 km/s). The intermediate-velocity second layer on Tib-8 may mark Cenozoic volcanic strata (Linzizong Formation) and/or substantially fractured and hydrothermally altered basement rocks underlying the Yangbajain/Damxung valleys (discussed in section 4.1). The underlying 5.7 km/s third layer on Tib-8 has velocities appropriate for granitic rocks, consistent with the bedrock geology of the Nyainqentanglha range, which borders the northern Yadong-Gulu rift.

Beneath Tib-2, Tib-4 and Tib-8, the base of the graben fill generally appears to deepen gently toward the east. Beneath Tib-10, it shows no obvious asymmetry. "Second-order" topography on the base of the graben fill is evident on all the profiles and likely reflects normal faulting of the buried basement surface. Tib-2 (Duoqen valley) shows the deepest basin, which thickens from about 500 m at the NW end of the line to about ~ 1.5 km on the SE end. Refraction calculations for Tib-4 (Nieru valley) also show a generally east thickening graben fill. Beginning at the west end of the line, refraction depths to the top of the basement deepen gradually from < 100 m. They

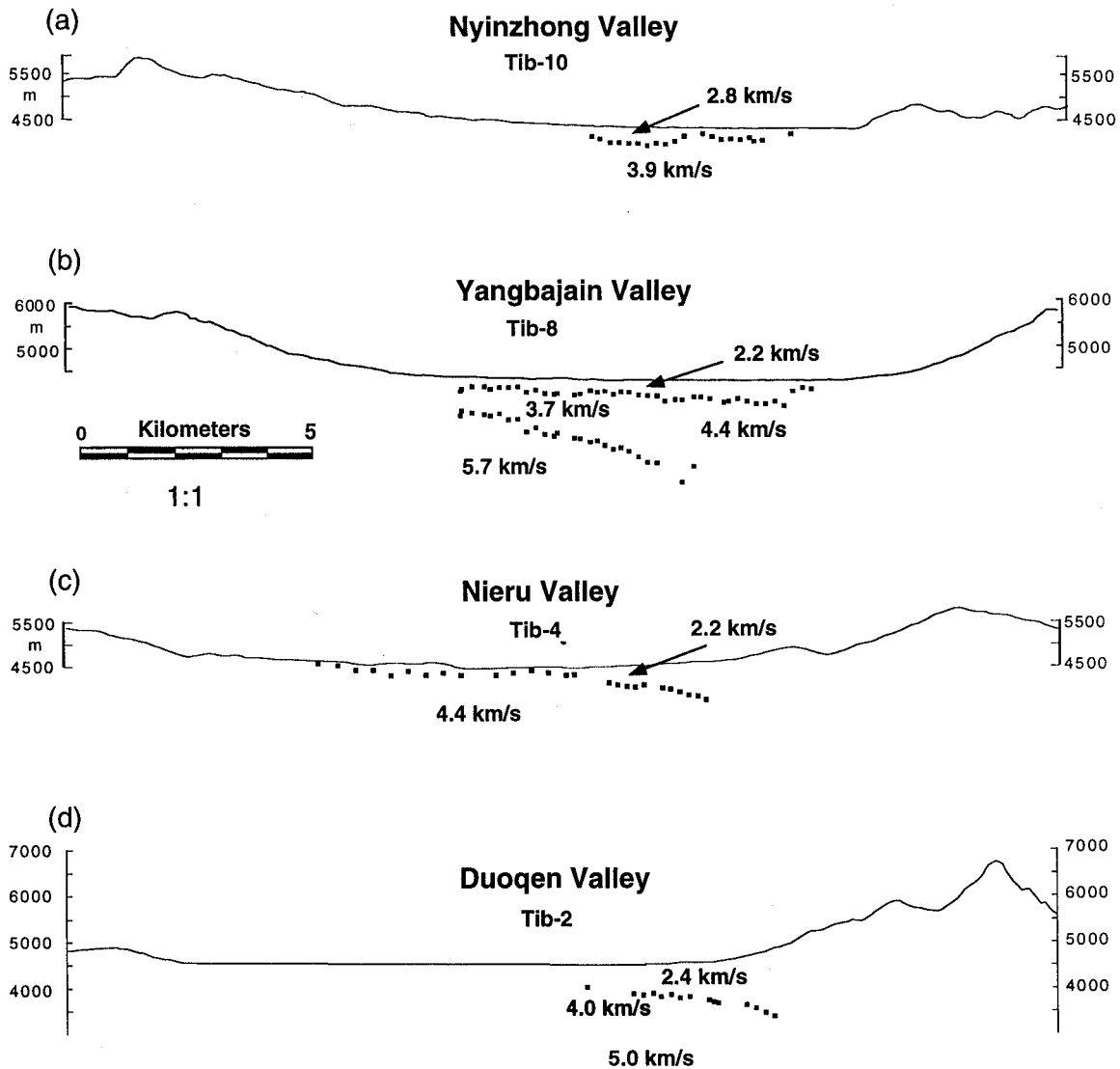


Figure 4. Refraction inverse depth calculations for individual shots plotted with topography at 1:1 scale for (a) Nyinzhong valley, (b) Yangbajain valley, (c) Nieru valley, and (d) Duoqen valley. Small squares are calculated basement depths.

then thin to ~100 m at ~5.0 km from the east end of the line. Farther east, the depth to the basement increases steadily to a maximum of ~800 m at the eastern terminus of the line.

The refraction model for Tib-8 shows generally eastward thickening graben fill. The fill thickens from ~150 m at the NW edge of the line to 800 m at the deepest point on the SE side (Figure 4b). Refraction depth calculations for the last three shots on line 8 show the basement refractor shallowing to the SE by ~500 m over a distance of less than 1.0 km. A deeper intrabasement refractor is also present over about three quarters of Tib-8. This refractor dips ~10° to the southeast, reaching a depth of ~2.2 km at ~7 km offset.

The graben fill on Tib-10 (Nyinzhong valley) appears to be substantially thinner than on the crosslines to the south. The top of the basement is an undulating surface with a maximum depth of ~500 m and a minimum of ~150 m.

These initial observations show that, in general, the base of the graben fill has a resolvable dip on the crosslines. This, in

turn, implies that the depth to basement determinations for the individual shots have some inherent error due to the horizontal layer assumption used in the inverse calculation. In order to estimate the likely size of this error, apparent velocities (V_1 and V_2) and the t intercept that would be yielded by an unreversed refraction experiment over a dipping layer were used to calculate an "apparent" depth to the basement, assuming a horizontal interface. The depth to the interface beneath the shot was varied between 0.1 and 1.5 km, and the dip of the interface was varied between 0° and 15°. These calculations showed that in the presence of a dipping layer, the horizontal layer solution systematically underestimates the actual depth to the refractor beneath the shot. Reference to Figure 4 suggests that the dip of the basement beneath the grabens is generally <10° (basement defined by interpolating picks). The depth error associated with a 10° dip is ~11%, corresponding to approximately 110-m error at 1.0 km depth and 11-m error at 100 m depth. This analysis implies that the simple one-dimen-

sional inverse determinations yield a good first approximation of the rift basin geometries.

3.2. Forward Modeling

To further constrain the basin fill geometry, forward modeling of the refracted arrivals was undertaken. Using MacRay™ software for the Macintosh, direct and refracted arrivals were generated for a specified geologic model. Plots of the synthetic travel time data were then compared to the observed travel time data for the recorded shots. Arrival times were picked using an automatic first-break picking module included in ProMAX™'s seismic data processing software package. This module takes a user-specified time gate and minimum-amplitude increase and searches each trace for the requisite jump in amplitude. The first large-amplitude gain is then chosen as the first break. The picks generated by the Pro-MAX™ module were visually edited for accuracy.

Two- and three-layer models were constructed in which the top surface was topography and successive layers were sub-horizontal to gently dipping horizons. Hand-picked interval velocities from individual shot files were used as a starting point for forward modeling. Initial layer thicknesses and dips for the forward models were estimated from the inverse models presented previously. A selection of five shots from each line, which provided overlapping coverage of the line, were forward modeled. For each of the selected shots, synthetic travel time curves were generated from the models and examined for visual correspondence to actual travel time curves. Layer thickness, velocity, and dip were varied iteratively to produce a "best fit" to the observed travel time curves. Figure 5 illustrates the degree or correspondence between the observed and synthetic travel time data generated by the best fit model for Tib-2, which is typical of the four lines. The best fit, forward models for each of the lines are shown in Figure 6, along with the initial inverse depth calculations and topography at 1:1 scale.

Because forward modeling is inherently nonunique, an attempt was made to estimate the likely error of the ray trace models. Using Tib-8 as a test example, layer thickness, depth, and dip were varied over small increments until there was a noticeable difference between the model and actual travel time curves. For depth-precision analysis, the undulating upper layer was incrementally moved up and down until obvious deviations from the data were apparent on the travel time curves. Velocity precision was estimated by incrementing layer velocities at 0.05-km/s intervals until the travel time curves were distinguishable from the best fit model travel time curve. Dip precision was estimated by varying the dip of the middle segment of the upper boundary on Tib-8. Owing to deviations from a horizontal layer at either end of the model, only the middle segment was altered to test dip sensitivity. Shot 37 from Tib-8, which most completely illuminates the middle segment, was used in the analysis. The analysis for Tib-8 suggests that, in general, the depth to the basement refractor can be determined to within ± 50 m, the velocity of the basement can be determined to within ± 0.2 km/s, and the dip of the basement can be determined to within $\pm 2^\circ$. The results of the forward modeling are described below.

3.2.1. Duoqen valley (Tib-2). Shots 2, 3, 4, 12, and 18 were modeled from line Tib-2 (Figure 6d). East traveling energy in shot 2 and west traveling energy in shot 4 constitute a reversed refraction survey. Second-order, high-frequency fluctuations in the observed first arrivals that cause mismatches with the synthetic curves can be attributed to inadequately corrected statics. The forward model that best fits the travel time curves for all of the shots modeled is a shallow (0.5-1.5 km thick) layer, the base of which is subhorizontal beneath the west end of the line and dips progressively more steeply to-ward the east. This top layer is interpreted to be Neogene-Quaternary basin fill with velocities ranging from 2.2 to 2.6 km/s (averaging ~ 2.4 km/s). The higher velocities in this range occur near the edges of the graben. Velocity variations

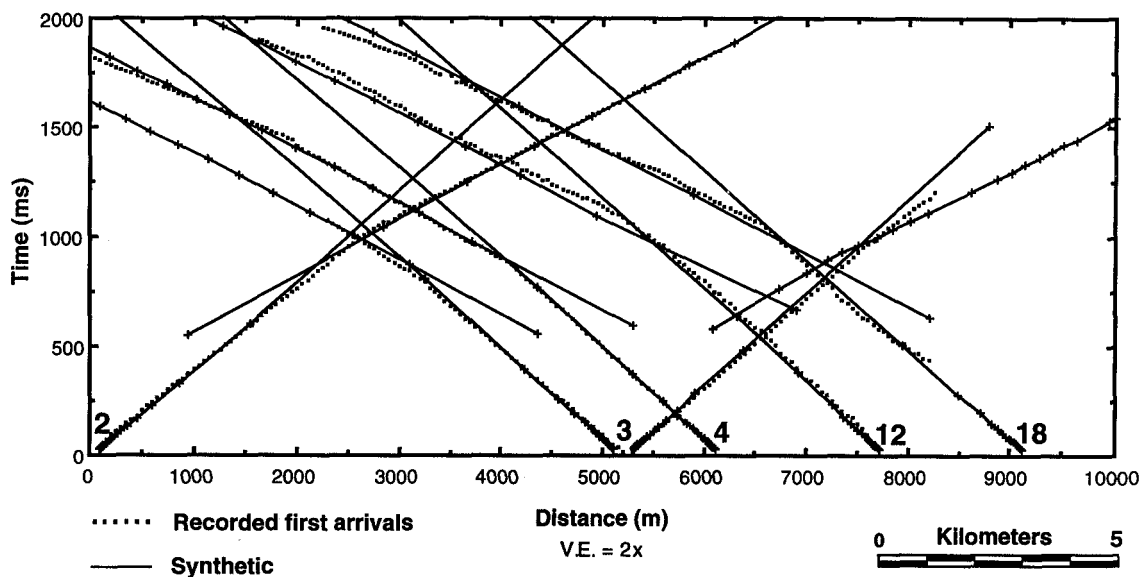


Figure 5. Comparison of observed travel times for Tib-2 first arrivals with those generated by best fit refraction model shown in Figure 6d.

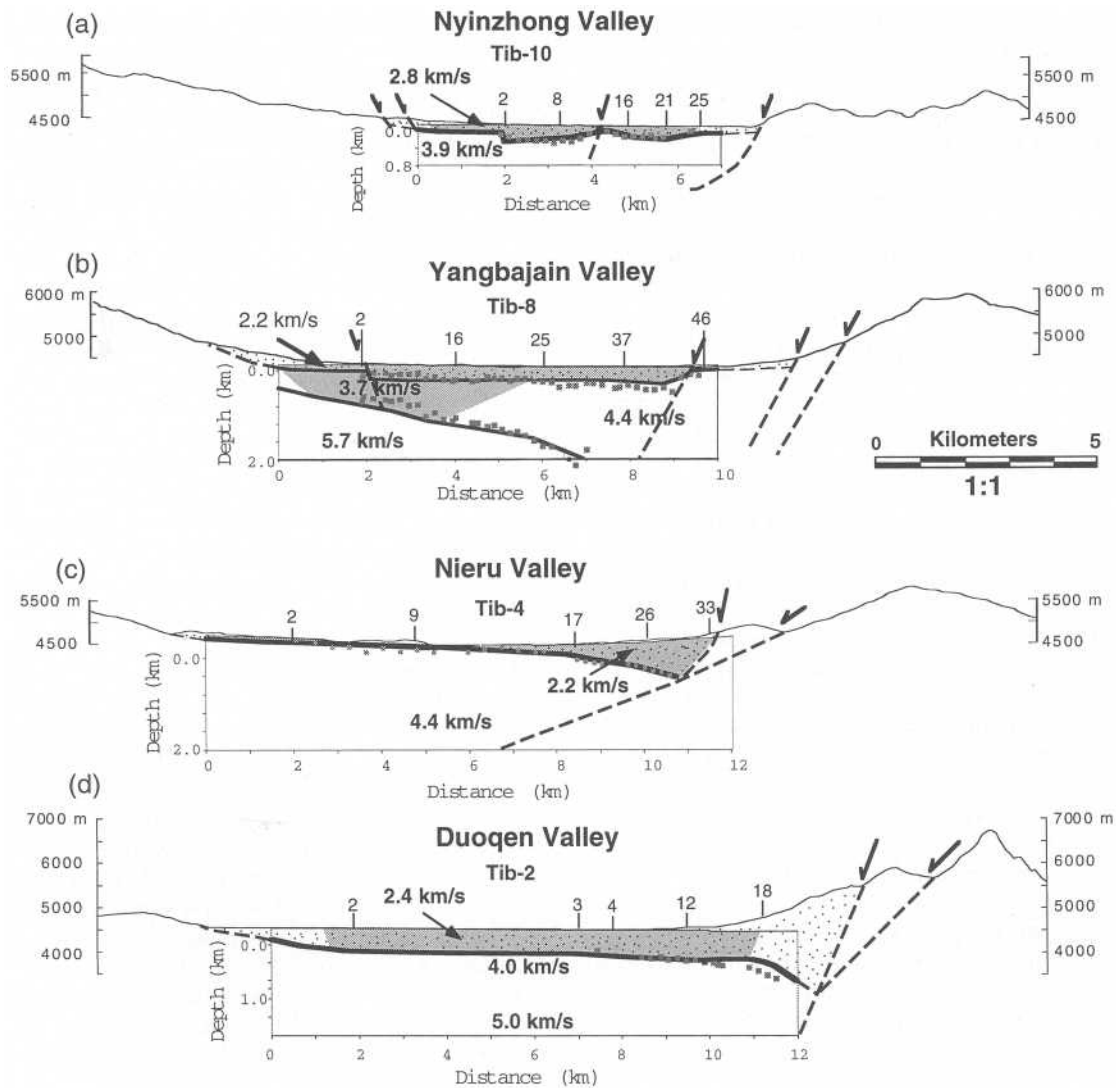


Figure 6. Best fit refraction models of shallow rift structure beneath INDEPTH crosslines for (a) Nyinzhong valley, (b) Yangbajain valley, (c) Nieru valley, and (d) Duoqen valley. Solid lines show forward model velocity boundaries; shaded squares indicate inverse depth calculations from Figure 4. Gray shading represents area illuminated by modeled shots. Stippled area shows interpreted extent of low-velocity graben fill.

within the basin fill may represent local sedimentary facies variations (conglomerate versus shale, amount of saturation, etc.) or variations in the degree of sediment compaction. A vertical velocity gradient is required within the basement (second layer) in order to produce emergent arrivals from the basement along the length of the profile (velocity increasing downward). The basement velocity also appears to increase slightly toward the SE from about 4.0 to 4.2 km/s. Data points from the initial inverse calculation for the depth to the base of the first layer match the forward model results within 100 m.

3.2.2. Nieru valley (Tib-4). In Nieru valley (Tib-4), shots 2, 9, 17, 26, and 33 were modeled (Figure 6c). Shots 2 and 17 constitute a reversed refraction traverse. The best fit model has an eastward thickening wedge of graben fill. The fill increases from < 100 m at the western side of the valley to ~250 m at 8.3 km from the west end of the line. Farther east, the graben fill

thickens more rapidly to ~1.4 km at 12 km from the west end of the line. The velocity structure is similar to that described for Duoqen valley (Tib-2), with top layer velocities increasing from west to east from 1.5 to 2.5 km/s (averaging ~2.2 km/s) and basement velocities increasing eastward from 4.0 to 4.5 km/s (averaging ~4.4 km/s). Initial inverse solutions for the base of the graben fill fall within 150 m of the ray trace model.

3.2.3. Yangbajain valley (Tib-8). For Tib-8, shots 2, 16, 25, 37, and 46 were modeled, with shots 2 and 25 constituting a reversed profile (Figure 6b). In contrast to the previously described crosslines, a three-layer solution was required to model the first arrival data for Tib-8, as shots 2, 16, and 25 exhibit a third, high-velocity leg to the refracted arrival. In the complete data set for Tib-8, the third leg shows up as far east as shot 33, ~7.3 km from the west end of the line. From NW to SE, the top layer deepens gently eastward to ~350 m depth at 2.0 km, where it then abruptly deepens. The abruptness of this

deepening suggests that it is fault produced. To the east, the base of the first layer continues subhorizontally until ~9.0 km from the west end of the line, where it abruptly shallows. This abrupt change in thickness is also interpreted to be fault produced. Velocities for the upper layer are consistently 2.2 km/s. Velocities for the second layer increase toward the SE from ~3.7 to 4.4 km/s. A vertical velocity gradient is required in this layer to produce emergent arrivals across the profile. The top of the third layer occurs at ~500 m depth at the NW end of the line and dips to the east to a depth of ~2.0 km at 7.0 km from the west end of the line, beyond which it is not illuminated. This layer has a velocity of 5.7 km/s at the top.

3.2.4. Nyinzhong valley (Tib-10). Shots 2, 8, 16, 21, and 25 were modeled for line Tib-10 (Figure 6a). Sources 2 and 25 represent a reversed refraction profile. The two-layer solution shows an upper layer with thickness varying between 100 and 400 m along the line. An abrupt thickening occurs at 2 km from the west end of the line where the upper layer doubles in thickness from 200 to 400 m. The abrupt change in thickness suggests that it is fault-related. A gradual eastward thinning of the upper layer occurs to ~4.3 km, east of which it thickens again slightly. Upper layer velocities vary between 2.5 and 3.0 km/s (averaging ~2.8 km/s), with lower velocities at the edges of the graben. The velocity in the underlying layer increases eastward from about 3.6 to 4.1 km/s (averaging ~3.9 km/s), and downward increasing velocity in this layer also appears to be required. Initial inverse depth calculations for the base of the graben fill fit the forward model within 100 m

3.3. Reflection Observations

As previously described, the field parameters for the survey were not optimized to image the upper few hundred meters to one km of the crust, and hence, for the most part, the shallow graben are not imaged on the CMP reflection sections. On Tib-4 and Tib-10, however, shallow intrabasement reflections are imaged that bear on the geologic interpretation of the rift structure discussed subsequently. These are shown in the reflection sections illustrated in Figure 7. Beneath Tib-4, an east dipping reflection is observed that projects upward toward the contact between crystalline rock (granite and granite gneiss) and overlying Tethyan sedimentary strata exposed on the east side of the Kangmar dome, immediately west of Nieru valley (KD in Figure 7). These reflections tie to reflections at ~1.0 s on Tib-3, the N-S line in Nieru valley, which toward the south project upward toward the Greater Himalayan belt/Tethyan belt contact exposed on the north flank of the Bhutan Himalaya [Hauck *et al.*, 1995]. We therefore interpret the east dipping reflections on Tib-4 as marking the top of the Greater Himalayan belt crystalline basement beneath Nieru valley.

Beneath Tib-10, an east dipping reflection is also observed, in this case projecting toward, and having an apparent dip comparable to, the NSZ cropping out in the Nyainqentanglha range immediately to the northwest (NSZ in Figure 7). Following Clark [1995], we interpret this reflection as marking the subsurface (southeastward) continuation of the NSZ.

4. Geologic Interpretation

Interpretative geologic cross sections across the Yadong-Gulu rift are shown in Figure 8. These incorporate the results of the seismic refraction analysis described above, seismic reflection data, published geologic mapping, and new geological observations of the INDEPTH field team. The sections are described from north to south, with the three sections crossing the Yangbajain/Damxung graben system, north of the suture, being grouped together as they exhibit a consistent structure.

4.1. Northern Yadong-Gulu Rift.

The sections crossing the Yangbajain/Damxung valleys incorporate three common elements (Figures 8a-8c): the shallow half-graben fill, as defined by the forward modeling of the first arrivals; the east dipping NSZ, as identified in outcrop along the eastern slope of the Nyainqentanglha range by Pan and Kidd [1992]; and the Paleozoic/Mesozoic sedimentary cover overlying the crystalline basement of the Nyainqentanglha range, as depicted on the 1:500,000 scale Academia Sinica/Royal Society Geotraverse map of Tibet [Kidd *et al.*, 1988]. Armijo *et al.* [1989, Figure 24a] have shown that the cover sequence is warped into a northwest facing syncline on the northwest side of the Nyainqentanglha range. At Nagen La, a very distinctive unconformity within the cover sequence, separating Cretaceous sedimentary strata above from underlying Paleozoic slates, is subvertical and northwest facing (INDEPTH field observations).

Figure 8a shows a section across the Damxung valley. The section runs NW-SE, approximately orthogonal to the trend of the valley, and crosses the Nyainqentanglha range at Nagen La. The NSZ is shown dipping ~30° to the southeast, consistent with its dip in outcrop where exposed farther south in the Nyainqentanglha range and with the position and dip of the NSZ reflection observed on Tib-10 to the south. The synclinally warped Paleozoic/Mesozoic cover strata on the west side of the range lie in the footwall of the NSZ, implying substantial rotation of the footwall of the NSZ during normal slip. The observation that rocks deformed at greater than 10 km depth are exposed in the footwall of the NSZ [Pan and Kidd, 1992; Harrison *et al.*, 1995], yet only a very shallow graben is developed in the hanging wall, implies that slip on the NSZ must have been accommodated at depth by lateral flow in the middle crust [e.g., Block and Royden, 1990] (discussed in section 5).

Figure 8b shows an interpretive section along Tib-10 in Nyinzhong valley. The general geometry and structural units are the same as those described above, with the exception that the denudation of the NSZ footwall is increasing to the south, as evidenced by the exposure of crystalline basement in the Nyainqentanglha range at this latitude. As in the north, the graben fill is only a few hundred meters thick, with the maximum thickness on the southeast side of the valley. The shallow basement reflections observed on Tib-10 that project upward toward the outcrop position of the NSZ constrain the subsurface position of the NSZ in the cross section.

The interpretation along Tib-8, still farther to the south, again shows the same general features, with incrementally

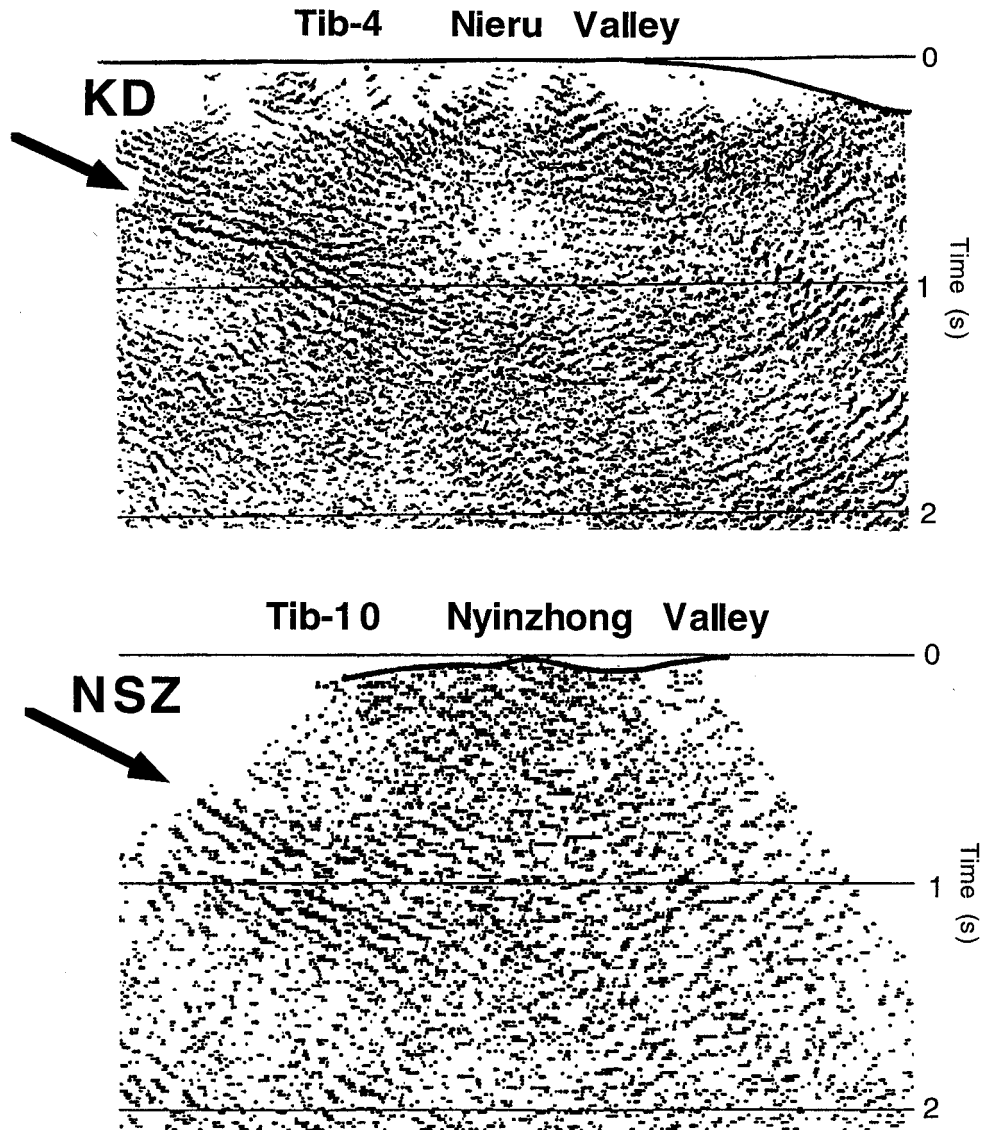


Figure 7. Migrated common midpoint seismic reflection sections for lines Tib-4 and Tib-10. The heavy line drawn across the top of the sections is the base of the Neogene-Quaternary graben fill interpreted from refraction analysis (see Figure 6). Dipping reflection labeled KD is the interpreted top of crystalline basement beneath Nieru valley (basement exposed in adjacent Kangmar dome); Dipping reflection labeled NSZ is the interpreted Nyainqentanglha Shear Zone reflection.

greater denudation of the NSZ footwall (Figure 8c). The graben fill reaches a maximum of a few hundred meters thickness along the southeast side of the valley. In this section, the relatively low "basement" velocities encountered immediately beneath the graben fill may be a consequence of active hydrothermal circulation in fractured bedrock beneath the graben or the local presence of relatively low-velocity volcanogenic strata beneath the graben fill. Tib-8 crosses through the Yangbajain geothermal field, an area of pronounced hydrothermal activity within the Yadong-Gulu rift and an area where exploration drilling for hydrothermal exploitation has revealed the presence of fragmental Cenozoic volcanics (rhyolite tuffs/breccias) in the floor of the graben [Cirenda *et*

al., 1987]. The third refractor, which is well-defined in the first arrival data on Tib-8, is interpreted as the top of Nyainqentanglha basement beneath the NSZ, consistent with the 5.7-km/s velocity associated with the refractor.

As noted above, *Harrison et al.* [1995] have published thermochronologic data constraining the evolution of the NSZ in the vicinity of Tib-10. These are the only such data that have been published for the Yadong-Gulu rift or, indeed, any of the rifts in Tibet. On the basis of their thermochronologic modeling results, *Harrison et al.* [1995] have argued that the NSZ initiated at 7.5 Ma (initiation of rapid cooling of the footwall) and that it was a relatively steep normal fault ($\sim 60^\circ$ dip) that penetrated to ~ 15 to 18 km depth. The geophysical

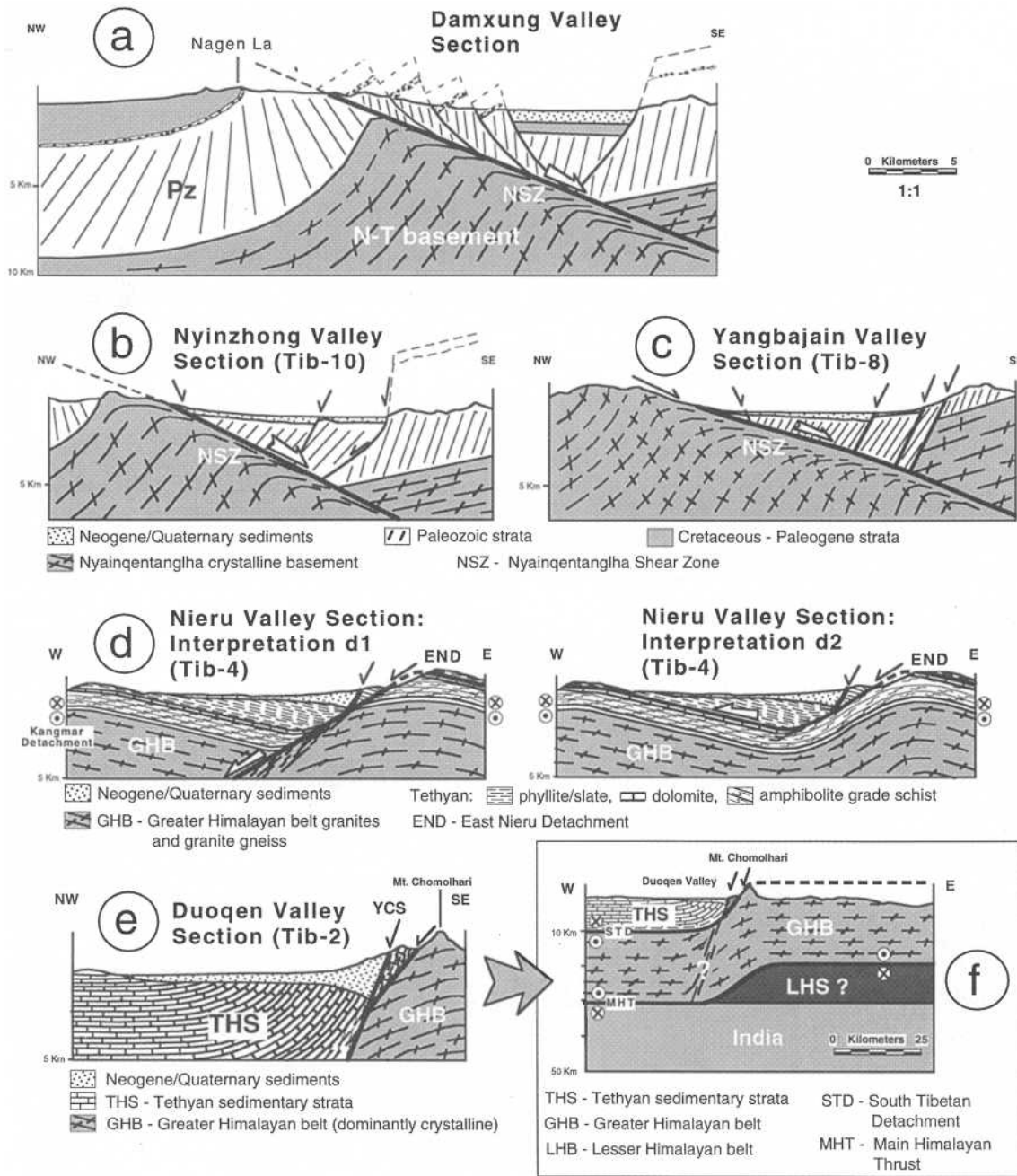


Figure 8. Interpretative geologic cross sections across the Yadong-Gulu rift: (a) Damxung valley section, (b) Nyinzhong valley section, (c) Yangbajain valley section, (d) Nieru valley section (two alternate interpretations), (e) Duoqen valley section, (f) Schematic small-scale section illustrating relationship of the Duoqen valley half graben to an interpreted lateral ramp in the Himalayan thrust system (see Wu et al., [this issue]).

and field geological data presented here, in contrast, imply that the NSZ is a shallow dipping fault, at least in the upper crust. The two data sets can be reconciled in a "rolling-hinge" model of crustal extension, such as has been proposed for a number of extensional detachments in the western United States [Spencer, 1984; Buck, 1988; Hamilton, 1988; Wernicke and Axen, 1988]. Applying the concept to the northern Yadong-Gulu rift, we suggest that the NSZ initiated with a steep dip through the upper crust (0-15 km) and that as slip

proceeded, midcrustal material flowed in beneath the footwall of the detachment to accommodate extension at depth (Figure 9). The progressive development of this geometry is such that material points in the footwall of the detachment would have been transported upward relative to the surface of the Earth and subsequently rotated around a horizontal axis that migrated with (behind) the receding hanging wall [e.g., Buck, 1988; Wernicke and Axen, 1988]. As with the analogous Basin and Range examples, the warping of the of the NSZ foot-

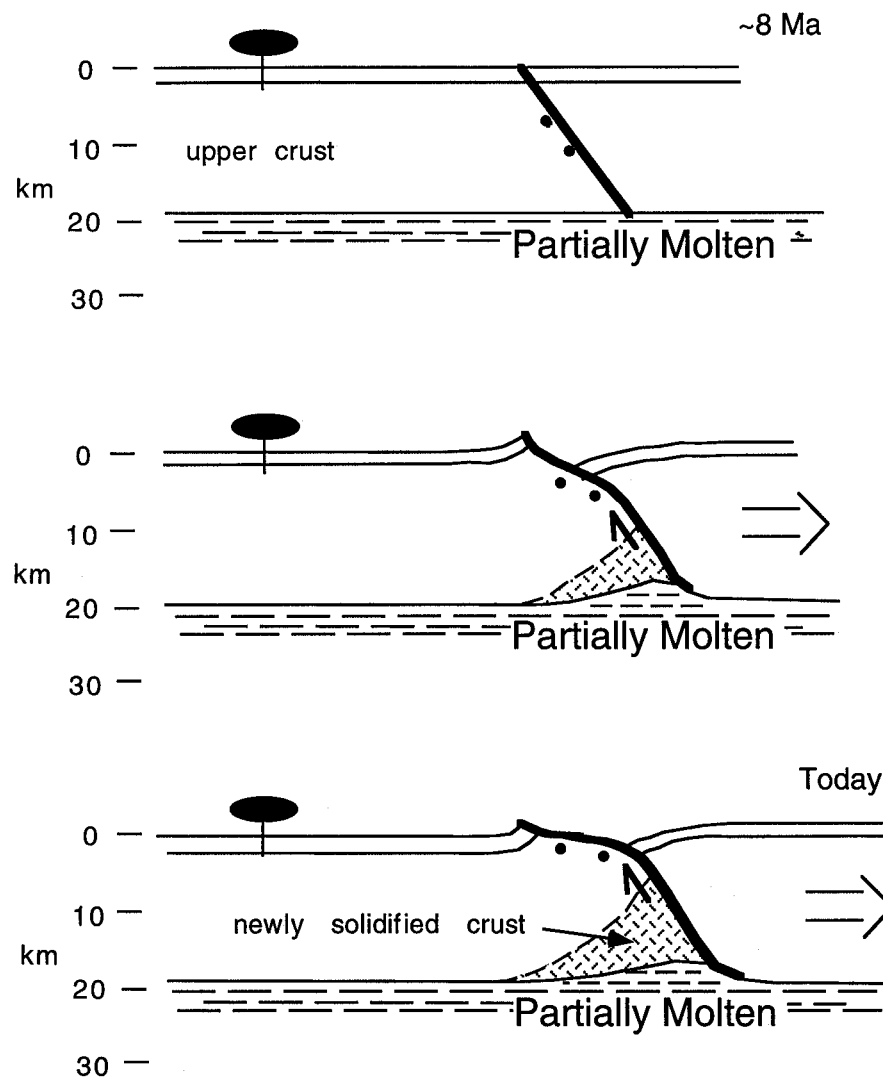


Figure 9. Schematic "rolling-hinge" model for the evolution of the northern Yadong-Gulu rift from (top) ~8 Ma to (bottom) the present. See text for discussion.

wall might have been accommodated by vertical simple shear in the footwall [Spencer, 1984] or flexural failure [Buck, 1988]. Additional structural observations within the Nyainqentanglha range are required to test these possibilities.

4.2. Southern Yadong-Gulu Rift.

The structure of the southern Yadong-Gulu rift (south of the Yarlung Zangbo) appears to be more variable than to the north and more obviously influenced by preexisting crustal structure. For Nieru valley, two alternate cross sections are presented (d1 and d2 in Figure 8). The principal elements of both are the shallow graben fill delineated by the refraction modeling, an approximately 3-km-thick Paleozoic/Mesozoic (Tethyan) sedimentary assemblage (preserved thickness), and the top-to-the-west normal-sense END, developed within Tethyan strata cropping out in the mountain range bordering the east side of Nieru valley.

The END, described by Kidd *et al.* [1995], is a several hundred meter thick (minimum) top-to-the-west ductile high-

strain zone capped by a several meter thick brittlely deformed, quartz-veined, carbonate/chlorite breccia horizon. It is exposed in several east-west trending valleys extending into the range on the east side of Nieru valley. The interpreted mylonitic footwall of the detachment (rocks underlying the breccia horizon) consists of an ~150-m-thick intensely sheared dolomite unit and underlying strongly foliated pelitic, carbonate, calcsilicate, and quartzofeldspathic schists. Mineral lineations and mechanical striations in the footwall rocks all trend east-west, and shear-sense indicators consistently indicate top-to-the-west transport. The attitude of the prominent foliation in the footwall rocks, as well as the outcrop pattern of the dolomite horizon indicate that the detachment is exposed in a domal culmination. The foliation exposed on the west flank of the culmination dips gently to moderately west. Black phyllites of probable Carboniferous age comprise the interpreted hanging wall of the detachment (above the breccia horizon).

Immediately west of Nieru valley, Tethyan sedimentary strata and underlying crystalline basement are exposed in the

Kangmar dome [Burg *et al.*, 1984]. Field geological investigation has shown that the lower part of the Tethyan assemblage exposed around the dome is ductily deformed with top-to-the-north sense of shear ("Kangmar detachment" [Chen *et al.*, 1990]). In interpretation d1 (Figure 8), the Nieru valley half graben is interpreted to have formed by normal slip on the END, which penetrates moderately steeply into the Greater Himalayan belt crystalline basement, subparallel to the easternmost brittle "range-front" normal fault cropping out along the east side of the valley. In this interpretation, normal slip on the END has produced roughly 3 km of throw (vertical off-set of the carbonate layer marking the top of the END) and roughly 5 km of horizontal extension (heave assuming an approximately 30° planar dip for the END as evidenced by observed dip of mylonitic foliation at the east side of the valley). In interpretation d2, the valley is also interpreted to have formed by slip on the END, but in this case the END is shown continuing westward in the subsurface along the top of the dolomite unit separating the Tethyan slates from underlying ductily deformed phyllites and schists. In this interpretation, the magnitude of E-W extension is unconstrained ($>=2$ km) but, in principle, could be very large. On the basis of the available field evidence, we prefer interpretation d1. In interpretation d2, top-to-the-west shear should be observed in the cover strata mantling the Kangmar dome, unless the top-to-the-north shear observed there postdates east-west slip on the END. This seems unlikely given the preponderance of regional geological and seismological data indicating that east-west extension is the latest (current) mode of deformation in southern Tibet [e.g., Mercier *et al.*, 1987].

The interpretative cross section for Duoqen valley (Tib-2) is shown in Figure 8e. The principal features of the Duoqen valley section are a shallow SE thickening wedge of graben fill material; Paleozoic/Mesozoic (Tethyan) sedimentary strata beneath the valley fill; granites and granitic gneisses of the Greater Himalayan belt forming the eastern graben-bounding mountains; and a thick (hundreds of meters) steeply west dipping mylonite zone, with down-to-west normal-sense shear exposed along the western flank of Mount Chomolhari. This mylonite zone was recognized during the INDEPTH field investigations. The mylonite zone trends parallel to the NNE trending Chomolhari range and coincides with the "Yadong cross structure", an apparent ~70-km left offset of the topographic crest of the Himalaya and South Tibetan Detachment System exposed along the north flank of the Himalaya [Burchfiel *et al.*, 1992]. On the basis of field observations in and around Duoqen valley, Wu *et al.* [this issue] have proposed that the Yadong cross structure is the surface manifestation of a large lateral ramp in the Himalayan thrust system (Figure 8f). This interpretation is based on (1) the observation that a substantial thickness of Tethyan strata (~9 km) is preserved to the west of and beneath Duoqen valley, whereas to the east the structurally underlying Greater Himalayan belt crystalline strata are widely exposed in Bhutan [Gansser, 1983]; (2) the existence of steeply west dipping Tethyan strata exposed on the west flank of Chomolhari (west facing monocline), which are ductily deformed in dip-slip (normal sense) shear and cut by a system of steep west dipping brittle normal faults; and (3) earthquake first-motion evidence for left-slip wrench faulting at depth beneath the southern continuation of

the Yadong cross structure [Wu *et al.*, this issue]. Combining the structural and geophysical observations, it appears that the Duoqen valley half graben is a shallow extensional basin superimposed on a large monoclinical flexure in the underlying Greater Himalayan/Tethyan thrust sheet caused by southward transport along a lateral ramp (Figure 8f). The E-W extension that produced the half graben could simply be a geometric consequence of the Tethyan/Greater Himalayan belt thrust sheet being transported southward onto the lateral ramp and/or may be related to general E-W extension of the Plateau.

5. Discussion

The observation of ductile normal faults exposing rocks exhumed from midcrustal depths (plastically deformed quartz) in the footwalls of three of the half grabens examined along the Yadong-Gulu rift implies that the rift as a whole may have accommodated substantially greater extension than previously thought. Currently, the only quantitative constraint on the magnitude of the slip for any of the rifts in Tibet comes from the thermochronologic work of Harrison *et al.* [1995], which indicates approximately 17 km of net vertical displacement on the NSZ during the past ~8 Myr. If the other rifts of southern Tibet are similarly bounded by ductile detachment faults, then the net east-west extension across the Tibetan Plateau may be an order of magnitude greater than suggested by Armijo *et al.* [1986]. Field geological and geochronological investigations of the other rifts in southern Tibet need to be undertaken to resolve this issue.

In the northern part of the Yadong-Gulu rift (Yangbajain/Damxung valley), the observation of the synclinal flexure on the west side of the Nyainqentanglha range and the shallow dip of the NSZ indicated by the field and reflection observations both imply substantial rotation of the NSZ footwall during normal slip. The geometric evolution is analogous to that which has been proposed for a number of extensional detachments in the western United States [Spencer, 1984; Buck, 1988; Hamilton, 1988; Wernicke and Axen, 1988]. As with those detachment systems, uplift and rotation of the detachment footwall during normal slip implies that material has flowed laterally at depth to accommodate the extension (flowed into the region beneath the footwall [Block and Boyden, 1990]). Both the very shallow depth of the Yangbajain/Damxung half graben and the small radius of curvature of the footwall flexure imply that the region of compensating flow must be within the crust. This accords with the observations of Masek *et al.* [1994], who inferred from the topography of the Tibetan rifts that flexural support of the rift bounding mountains in Tibet is restricted to the upper crust. The combined results indicate that, at least in the vicinity of the northern Yadong-Gulu rift, the middle crust has flowed to accommodate opening of the rift, effectively behaving as a fluid on the timescale of the extensional deformation (of the order of 10 Myr).

Observations from the larger INDEPTH data set suggest that this fluid behavior may be a consequence of the middle crust being partially molten [Nelson *et al.*, 1996]. The southern Tibetan Plateau is a region of elevated heat flow, as manifested by the widespread occurrence of hot springs [Cirenda *et al.*, 1987], and locally extreme heat flow has been measured within the Yadong-Gulu rift in Yamdrok Tso (Yamdrok lake)

(average 146 mW/m² [Francheteau *et al.*, 1984]). The INDEPTH seismic reflection profiles extending along the Yadong-Gulu rift show a prominent, undulatory, reflection horizon at 15-20 km depth, which extends from the vicinity of Yamdrok Tso to the north end of the survey. This reflection band locally exhibits anomalously high amplitude and negative polarity [Brown *et al.*, 1996] and, at wide-angle, strong *P*-to-*S* conversion [Makovsky *et al.*, 1996], properties suggestive of local occurrences of a solid-over-fluid interface coinciding with the reflecting horizon. Receiver function analyses of INDEPTH teleseismic data show a marked low-velocity zone within the crust beneath the northern Yadong-Gulu rift, the top of which broadly coincides with the 15-20 km deep reflection band [Kind *et al.*, 1996]. The low-velocity zone extends southward in the subsurface to approximately the Yarlung Zangbo, south of which it appears to die out. New magnetotelluric (MT) sounding data indicate that anomalously electrically conductive crust exists at depth beneath the entire northern two thirds of the INDEPTH survey (north of the Kangmar dome), beginning at a depth of a few tens of kilometers [Chen *et al.*, 1996]. Additionally, the new MT data indicate that the highly electrically conductive crust at a few tens of kilometer depth extends outside the northern Yadong-Gulu rift, both to the northwest and southeast. These observations, combined with published thermal modeling results [e.g., England and Thompson, 1986], have led to the suggestion that the 15-20 km-deep reflection horizon imaged on the CMP profiles marks the top of a midcrustal partial-melt layer underlying the southern Tibetan Plateau that has been produced by convergent crustal thickening [Nelson *et al.*, 1996]. Lateral flow in this partially molten layer can accommodate the opening of the Tibetan rifts in the manner depicted schematically in Figure 9. As extension proceeds across a "Nyainqentanglha-type" detachment fault, the partially molten middle crust would be expected to flow in beneath the rising footwall and be progressively accreted (frozen) to it as the footwall rises.

6. Conclusion

The Yadong-Gulu rift, one of the largest of the extensional rift systems on the southern Tibetan Plateau, is composed of a number of shallow half grabens. The Neogene-Quaternary fill of these shallow basins reaches a maximum thickness of ~1.5 km in the southern part of the rift but averages only a few hundred meters thickness along most of the rift. At several locations along the rift, normal-sense, ductile high-strain zones that expose rocks deformed in the midcrust have been observed. In the northern Yadong-Gulu rift, the footwall of the rift also appears to be strongly rotated. The combined geophysical and geological observations imply that the northern Yadong-Gulu rift is extending in a fashion analogous to that of the core complexes of the western United States. In particular, uplift and rotation of the footwall of the rift is being accommodated at depth by flow in the middle crust. It is likely that the middle crust is partially molten. In the southern part of the Yadong-Gulu rift, the bounding ductile high strain-zones are moderate to steeply dipping, and the half grabens are also very shallow features. The half grabens there appear to be superimposed on pre-existing collisional structures, in particular, a monoclinical flexure formed over a large lateral ramp in the Himalayan thrust system. If the structure of the other rifts in Tibet is similar to the Yadong-Gulu rift, the crust beneath the plateau may have experienced substantially more east-west extension than previously thought.

Acknowledgments. This work was undertaken as part of Project INDEPTH which was supported jointly by the U.S. National Science Foundation Continental Dynamics Program, Ministry of Geology and Mineral Resources of China, and the Chinese National Science Foundation. We are particularly grateful to Zhao Wenjin, leader of the Chinese INDEPTH team, whose many efforts in China have made INDEPTH possible. Support for Syracuse University personnel was provided by NSF grants EAR-9316132 and EAR-9316569. The authors gratefully acknowledge the constructive advice about and criticisms of an earlier version of this paper by Gary Axen and Lothar Ratschbacher.

References

- Alsdorf, D., L.D. Brown, and K.D. Nelson, Possible upper mantle reflection fabric on seismic profiles from the Tethyan Himalaya: Identification and tectonic interpretation, *J. Geophys. Res.*, **101**, 25,305-25,320, 1996.
- Armijo, R., P. Tapponnier, J.L. Mercier, and H. Tong-Lin, Quaternary extension in southern Tibet: Field observations and tectonic implications, *J. Geophys. Res.*, **91**, 13,803-13,872, 1986.
- Armijo, R., P. Tapponnier, and H. Tong-Lin, Late Cenozoic right-lateral strike-slip faulting in southern Tibet, *J. Geophys. Res.*, **94**, 2787-2838, 1989.
- Block, L., and L.H. Royden, Core complex geometries and regional scale flow in the lower crust, *Tectonics*, **9**, 557-567, 1990.
- Brown, L.D., W. Zhao, K.D. Nelson, M. Hauck, D. Alsdorf, A. Ross, M. Cogan, M. Clark, X. Liu, and J. Che, Bright spots, structure, and magmatism in southern Tibet from INDEPTH seismic reflection profiling, *Science*, **274**, 1688-1690, 1996.
- Burchfiel, B.C., Z. Chen, L.H. Royden, Y. Liu, and C. Deng, Extensional development of Gabo valley, southern Tibet, *Tectonophysics*, **194**, 187-193, 1991.
- Burchfiel, B.C., Z. Cheng, K.V. Hodges, Y. Liu, L.H. Royden, C. Deng, and J. Xu, The South Tibetan detachment system, Himalayan orogen: Extension contemporaneous with and parallel to shortening in a collisional mountain belt, report, 41 pp., Geol. Soc. of Am., Boulder, Colo., 1992.
- Burg, J.P., M. Guiraud, G.M. Chen, and G.C. Li, Himalayan metamorphism and deformations in the North Himalayan belt (southern Tibet, China), *Earth Planet. Sci. Lett.*, **69**, 391-400, 1984.
- Buck, W.R., Flexural rotation of normal faults, *Tectonics*, **7**, 959-973, 1988.
- Chen, L., J.R. Booker, A.G. Jones, N. Wu, M.L. Unsworth, W. Wei, and H. Tan, Electrically conductive crust in southern Tibet from INDEPTH magnetotelluric surveying, *Science*, **274**, 1694-1696, 1996.
- Chen, Z., Y. Liu, K.V. Hodges, B.C. Burchfiel, L.H. Royden, and C. Deng, The Kangmar dome: A metamorphic core complex in southern Xizang (Tibet), *Science*, **250**, 1552-1555, 1990.
- Cirenda, D. Wang, and C. Qin, *Yangbajain Geothermal Field in Xizang (Tibet)*, 140 pp., Xizang People's Publ. House, Lhasa, China, 1987.
- Clark, M.K., Nature of the Nyainqentanglha Shear Zone at depth from INDEPTH seismic experiments: Low-angle detachment faulting and metamorphic core complex analog in southern Tibet, 50 pp., B.S. thesis, Cornell Univ., Ithaca, New York, 1995.
- England, P., and G. Houseman, Extension during continental convergence, with application to the Tibetan plateau, *J. Geophys. Res.*, **94**, 17,561-17,579, 1989.
- England, P., and A. Thompson, Some thermal and tectonic models for crustal melting in continental collision zones, in *Collision Tectonics*, edited by J.G. Ramsey, M.P. Coward, and A.P. Ries, *Geol. Soc. Spec. Publ.*, **19**, 83-94, 1986.
- Fielding, E.J., B.L. Isacks, M. Barazangi, and C.C. Duncan, How flat is Tibet?, *Geology*, **22**, 163-167, 1994.
- Francheteau, J., C. Jaupart, J.S. Xian, K. Wen-Hua, L. De-Lu, B. Jia-Cha, W. Hung-Pin, and D. Hsia-Yeu, High heat flow in southern Tibet, *Nature*, **307**, 32-36, 1984.
- Gansser, A., *Geology of the Himalayas*, 289 pp., Wiley-Interscience, New York, 1964.
- Gansser, A., *Geology of the Bhutan Himalaya*, 181 pp., Denkschr. Schweiz. Naturforsch. Ges. **96**, 1983.
- Hamilton, W.B., Detachment faulting in the Death valley region, California and Nevada, *U.S. Geol. Surv. Bull.*, **1790**, 51-85, 1988.
- Harrison, T.M., P. Copeland, W.S.F. Kidd, and A. Yin, Raising Tibet, *Science*, **255**, 1663-1670, 1992.

- Harrison, T.M., P. Copeland, W.S.F. Kidd, and O.M. Lovera, Activation of the Nyainqentanglha Shear Zone: Implications for uplift of the southern Tibet Plateau, *Tectonics*, *14*, 658-676, 1995.
- Hauck, M.L., K.D. Nelson, C. Wu, M.J. Cogan, L.D. Brown, W.S.F. Kidd, M.E. Edwards, J.T. Kuo, and W. Zhao, Ramping of the Main Himalayan Thrust and development of the South Tibetan Detachment and Kangmar basement dome: INDEPTH reflection profiles in southern Tibet, *Geol. Soc. Am. Abstr. Programs*, *27*, A-336, 1995.
- Kidd, W., M. Edwards, Y. Yue, C. Wu, and K. Nelson, The END (East Nieru Detachment): A new low-angle mylonitic shear zone bordering the Yadong-Gulu rift system, southern Tibet, *Geol. Soc. Am. Abstr. Programs*, *27*, A-337, 1995.
- Kidd, W.S.F., Y. Pan, C. Chang, M.P. Coward, J.F. Dewey, A. Gansser, P. Molnar, R.M. Shackleton, and Y. Sun, Geological mapping of the 1985 Chinese-British Tibetan (Xizang-Qinghai) Plateau Geotransverse route, *Philos. Trans. R. Soc. London, Ser. A*, *327*, 287-305, 1988.
- Kind, R., J. Ni, W. Zhao, J. Wu, X. Yuan, L. Zhao, E. Sandvol, C. Reese, J. Nabelek, and T. Hearn, Mid-crustal low velocity zone beneath the southern Lhasa block: Results from the INDEPTH-II Earthquake recording program, *Science*, *274*, 1692-1694, 1996.
- Liu, Z. Q., *Geologic map of the Qinghai-Xizang Plateau and its Neighboring Regions*, scale 1: 1, 500,000, Chinese Acad. of Geol. Sci. Geol. Publ. House, Beijing, 1988.
- Makovsky, Y., S.L. Klempner, L. Ratschbacher, L.D. Brown, M. Li, W. Zhao, and F. Meng, INDEPTH wide-angle reflection observation of P-wave-to-S-wave conversion from crustal bright spots in Tibet, *Science*, *274*, 1690-1691, 1996.
- Maluski, H., P. Matte, M. Brunel, and X. Xiao, Argon 39 - Argon 40 dating of metamorphic and plutonic events in the North and High Himalayas belts (southern Tibet-China), *Tectonics*, *7*, 299-326, 1988.
- Masek, J.G., B.L. Isacks, E.J. Fielding, and J. Browaeys, Rift-flank uplift in Tibet: Evidence for a viscous lower crust, *Tectonics*, *13*, 659-667, 1994.
- Mercier, J., R. Armijo, P. Tapponnier, E. Carey-Gailhardis, and H. Tong Lin, Change from Late Tertiary compression to Quaternary extension in southern Tibet during the India-Asia collision, *Tectonics*, *6*, 275-304, 1987.
- Molnar, P., and P. Tapponnier, Active tectonics of Tibet, *J. Geophys. Res.*, *83*, 5361-5375, 1978.
- Molnar, P., P. England, and J. Martinod, Mantle dynamics, uplift of the Tibetan plateau, and the Indian monsoon, *Rev. Geophys.*, *31*, 357-396, 1993.
- Nelson, K.D., et al., Partially molten middle crust beneath southern Tibet: A synthesis of Project INDEPTH results, *Science*, *274*, 1684-1687, 1996.
- Pan, Y., and W.S.F. Kidd, Nyainqentanglha Shear Zone: A late Miocene extensional detachment in the southern Tibet Plateau, *Geology*, *20*, 775-778, 1992.
- Press, F., Seismic velocities, in *Handbook of Physical Constants*, edited by S.P. Clark, Jr., *Geol. Soc. Am. Mem.*, *97*, 97-173, 1966.
- Ratschbacher, L., W. Frisch, G. Liu, and C. Chen, Distributed deformation in southern and western Tibet during and after the India-Asia collision, *J. Geophys. Res.*, *99*, 19,917-19,945, 1994.
- Searle, M., et al., The closing of Tethys and the tectonics of the Himalaya, *Geol. Soc. Am. Bull.*, *98*, 678-701, 1987.
- Spencer, J.E., The role of tectonic denudation in the warping and uplift of low-angle normal faults, *Geology*, *12*, 95-98, 1984.
- Tapponnier, P., G. Peltzer, and R. Armijo, On the mechanics of collision between India and Asia, in *Collision Tectonics*, edited by J.G. Ramsey, M.P. Coward, and A.P. Ries, *Geol. Soc. Spec. Publ.*, *19*, 115-157, 1986.
- Wernicke, B., and G.J. Axen, On the role of isostasy in the evolution of normal fault systems, *Geology*, *16*, 848-851, 1988.
- Wu, C., K.D. Nelson, G. Wortman, S.D. Samson, Y. Yue, J. Li, W.S.F. Kidd, and M.E. Edwards, Yadong cross structure and South Tibetan Detachment in the east central Himalaya (89°-90°E), *Tectonics*, this issue.
- Zhao, W., K.D. Nelson, and Project INDEPTH Team, Deep seismic reflection evidence for continental underthrusting beneath southern Tibet, *Nature*, *366*, 557-559, 1993.
- D. Alsdorf, L.D. Brown, M. Clark, M.L. Hauck, Institute for the Study of the Continents, Cornell University, Ithaca, NY 14853.
- K.D. Nelson and Changde Wu, Department of Earth Sciences, Syracuse University, Syracuse, NY 13244. (e-mail: kdnelson@symbolmailbox.syr.edu)
- M.J. Cogan, Schlumberger Geco-Prakla, 1325 Dairy Ashford, Houston, TX 77077. (e-mail: mjcogan@symbolpop3.wt.net)
- M.A. Edwards and W.S.F. Kidd, Department of Earth and Atmospheric Sciences, SUNY at Albany, Albany, NY 12222.
- J.T. Kuo, Aldridge Laboratory of Applied Geophysics, Columbia University, New York, NY 10027.
- J. Li, Y. Yue, and W. Zhao, Chinese Academy of Geological Sciences, Baiwanzhuang Road 26, Beijing, China.
- Additional members of the Project INDEPTH Team contributing to this research include: Wenjin Zhao, Yongjun Yue, Jixiang Li, Chinese Academy of Geological Sciences; L.D. Brown, M.L. Hauck, D. Alsdorf, M. Clark, Institute for the Study of the Continents, Cornell University; M.A. Edwards, Department of Earth and Atmospheric Sciences, SUNY at Albany; J. T. Kuo Aldridge Laboratory of Applied Geophysics and Lamont-Doherty Earth Observatory of Columbia University.

(Received December 3, 1996;
revised October 17, 1997;
accepted October 27, 1997.)